Quantification of Grid Discretization Effects in Presence of Realistic Geological Heterogeneities

H. Nguyen, C. V. Deutsch, and R. Bentsen
School of Mining and Petroleum Engineering
University of Alberta, Edmonton, Alberta

Grid discretization has an effect on reservoir characterization. This paper describes procedures to quantitatively assess grid discretization effects and uncertainty in reservoir modeling as well as a fast ranking technique to assess geological uncertainty.

INTRODUCTION

Reservoir characterization and model selection are very important steps. One of the main purposes of reservoir characterization is to capture the geologic and petrophysical features that affect reservoir flow mechanisms. The geological model must be able to capture features that directly affect flow. Reservoir Characterization forms the foundation for the other reservoir modeling and simulation steps. Hence, any error in reservoir characterization can be costly in terms of engineering results.

Another important step in reservoir modeling is to choose the fluid flow simulation model that is best suited to the objectives of the simulation. For a specific simulation task, various simulation models can be used. Each simulation model has certain advantages and disadvantages. Time and cost considerations and computer and labor resources must be taken into account in the final decision. Grid selection is an important component in model selection. The dimensionality of the model and the well spacing of the reservoir define the resolution required. The resolution dictates the number and coarseness of the cells. Computer resources are limited. Grid determination is an iterative process that balances available computing capacities and modeling needs.

Reservoir parameters such as vertical and horizontal permeability, relative permeability, and porosity depend on model cell dimensions [1]. These properties are often obtained on a different scale; therefore, the scaling of the available data to the model cell dimensions becomes important. The reservoir may be discretized very finely for geostatistical modeling so that petrophysical data as well as different geological trends and features are better represented. Most flow simulators cannot handle such fine grid systems. Thus, upscaling is necessary.

There are different methods for upscaling. One problem in the upscaling process is that extreme high and low values may be diluted and lost; therefore, the heterogeneous character of the reservoir may not be fully described and the result may be the introduction of error into the reservoir performance predictions. Choosing the right scaling techniques and parameters can result in a better prediction of reservoir flow behavior.

This study examines how grid sizes and data scaling affect the reservoir description process, and how information on heterogeneity may be lost as a result of an increase in grid size. From this grid sensitivity study, the uncertainty associated with combining effects of geological realizations and grid sizes is assessed quantitatively.

Three major steps were involved in this study: (1) construction of geological models using geostatistical modeling techniques, (2) upscaling of the geostatistical models, and (3) flow simulation runs to see the effects of different geological realizations on the flow performance of the reservoir.

Data used for this study were from the two wells drilled 600 m from each other; they intersect an approximately 100 m thick reservoir. Only the porosity and permeability data were analyzed. The porosity was measured at 0.1m intervals over the entire reservoir thickness. The permeability was measured irregularly, but tabulated in the same depth interval as the porosity.

GEOSTATISTICAL MODELING USING WINGSLIB

Reservoir size in this study is 600 m long, 1 m wide and 100 m depth (2 D problem). Porosity is simulated using Sequential Gaussian Simulation. Permeability is simulated using SGS collocated cokriging option with porosity as a constrained data. Figure 1 illustrates a permeability distribution from geological realization 1 simulated at 128 x 1 x 96 grid. The size of grid can be found in Table 1.

FLOW SIMULATION USING ECLIPSE

The system consists of two wells, one of which (well No.1) was an injection well, and one of which was a production well (well No. 2). The depth to the top of the reservoir was set at 2000 m. The pressure at this point (reference depth) was 100 bars. A two-phase problem, water and oil, was considered. The initial water saturation was 25 % and the injection rate was 100 m^3/day. The BHP for the injector was kept under 500 bars. The minimum BHP of the injector was kept above 20 bars. The limiting oil production rate was 1 m^3/d. In order to see the effects of discretization on the flow of fluids with different properties, three oils with different viscosities were considered for the simulation. Thus, there were displacements with three different mobility ratios: favorable (M = 0.4), unit (1) and unfavorable (M = 1.8).

The well performance parameters recorded were: oil and water production rates (WOPR, WWPR), total oil and water produced (WOPT, WWPT), oil recovery efficiency (FOEW), water cut (WWCT), reservoir volume injected water (WVIW), and reservoir pore volume (FRPV). The water injected measured in pore volumes (PVWI) was calculated by dividing WVIW to FRPV. The new "oil rate" normalized to PVWI was defined using the cumulative oil production data, for each simulation time step ΔWOPT/ΔPWWI. Similarly, the new "water rate" was defined as ΔWWPT/ΔPVWI.

SIMULATION OF A HOMOGENEOUS RESERVOIR

In order to see the effects of discretization alone, the flow performance of a homogeneous reservoir was simulated. The reservoir simulated was assumed to be homogenous and isotropic. The average reservoir porosity 0.17 was calculated by arithmetic averaging of the porosity values from the well data. The geometric average permeability was 322.1 mD. Several different reservoir discretizations were implemented. The cell sizes used are shown in Table 2. The wells go through the centers of the first and last cells in the x direction.

Two parameters were monitored: the recovery factor at one pore volume water injected (1 PVWI) and the time to breakthrough for the different mobility ratios. Plots of the results are illustrated in Figure 2. The runs for the last two grid systems were very slow and did not converge. Only one run for the 241 x 200 grid, with a favorable mobility (M = 0.4), finished successfully.

In Figure 2, the recovery factors (RFs) calculated at 1 PVWI (a) and the breakthrough times (BTs) (b) are plotted versus the number of cells on a logarithmic scale. For all three mobility

ratios, the RF increases as the number of cells increases. It was obvious that the higher the mobility ratio, the smaller the amount of oil produced at 1 PVWI. On the other hand, the RF ranges for different mobility ratios were slightly different, larger for M = 0.4 and smaller for M = 1.8. As a result of this, the slope of the RF curve is larger for the M = 0.4 case than it is for the M = 1.8 case. From Figure 2(a), convergence behavior associated only with discretization is observed for all mobility ratios. In order to quantify the difference in the RFs, the RFs of the finest grid was assumed to be the true value and the percentage differences with respect to the other grids were calculated. The percentage differences between the different mobility ratios were very similar, although the absolute values were very different. A maximum difference of around 4-5 % occurs at the coarsest grid. The difference decreases as the grid gets finer.

Breakthrough is considered to occur when the water cuts reach ≈ 0.01. In some cases, it was difficult to locate the exact breakthrough time, because the water cut increased sharply over one time step. The BT was measured in PVWI (Figure 2(b)). The trend was that the higher the mobility ratio, the earlier the BT. It appears that, even for a homogenous reservoir, in the case of an unfavorable displacement, viscous fingering may take place. There is an indication of convergence for M = 0.4, but it is harder to predict the behavior of the other mobility ratios as the grid system gets finer. As Figure 2(b) shows, for M = 1, the BTs increase significantly for the first three coarse grids, then flatten out for the last two finer grids. For the case of M = 1.8, the picture is more complicated. The BT times increase for the first two coarse grids, and then decrease, as the grids get finer. Maybe, for different grids, the water channels differently. Different paths lead to different BTs. Similar to the way used for the RFs, the difference between the BTs for the finest grid and for the other grids was calculated. Unlike the RF, there was a very big difference in BT between different grids, up to 30% in the case of the coarsest grid. The unfavorable mobility ratio case shows unpredictable behavior. The reason for this was explained earlier.

POROSITY AND PERMEABILITY SCALING

There were two types of scaling. The first type is downscaling, where the original data have a larger support volume and data at a finer scale are obtained. The second type is upscaling, where data from small supporting volumes have to be averaged to obtain representative values for a bigger volume. Depending on the nature of the data, one of two approaches can be applied. In this study, two scaling approaches were considered

The reservoir was simulated geostatistically at a very coarse scale of 8 x 1 x 6. Five grid systems were considered starting with an 8 x 6 grid and finishing with a 128 x 96 grid (2-D problem). The cell sizes for these grids can be seen in Table 1. The porosity and permeability for the finer grids were obtained from a scale down of the data for the coarsest 8 x 6 grid. Each data point from the 8 x 6 grid was assigned to four cells of the next finer grid (16 x 12). The data for the next finer grid (32 x 24) was obtained similarly from the 16x12 grid.

The RFs and BT times for all of the simulated grids are compared. Recovery values for all of the grids are lower than the corresponding ones for the homogeneous cases. There is an indication of convergence as the RFs and BTs increase gradually as the number of cells increases. The differences, for various grid sizes, in RFs and BTs were compared with the results for the finest grid size. The general trend is that the coarser grid, the bigger the difference from the reference values. The RF for M = 0.4 curve shows the greatest difference, reaching 8 % for the 8 x 6 grid. For M = 1 and 1.8, the values are close to each other and lower than the M = 0.4 curve, reaching a 6 % difference from the finest grid for the 8 x 6 grid. The BT times exhibit an even larger difference. The biggest difference was 37% for M = 1, and the 8 x 6 grid.

One important consideration in the description of a heterogeneous reservoir is the problem of averaging from one scale to another. Averaging means finding a unique value for the bigger volume that is representative of the set of smaller measurements that can be obtained and processed within it [2]. For different variables, different averaging approaches should be applied. If the variables are additive, such as porosity or saturation, a simple arithmetic averaging can be applied. However, there are other parameters, such as permeability and mobility, that are not additive; therefore, arithmetic averaging cannot be used. Different methods can be found in the literature. Only averaging techniques for permeability are addressed here: power averaging and flow-based averaging techniques.

Power law averaging has been used extensively in research work on upscaling, in recent years. Journel et al. [2] stated that, for a rock with a shale content p of less than 0.5, the power average provides a good fit to the curve of effective permeability (k_{eff}) versus p. The average power was determined empirically. Deutsch [3] suggests an exponent range of 0.5 to 1 in the horizontal x and y directions. For the vertical direction, the range should be from -1 to 0. For the two well data set, a w-value of 0.6 was chosen for the x and y directions and a value of -0.5 for the z direction.

An accurate way of calculating the effective permeability of large coarse-grid blocks containing many fine-grid blocks is to solve flow equations with constant pressure and no-flow boundary conditions, or periodic boundary conditions. However, using this approach requires extensive computation. This approach is referred to by many researchers as the pressure solver technique, because the approach solves for the fine-grid pressure distribution first and then calculates the effective permeability using the calculated pressure drops and fluxes and Darcy's equation [4].

The power and flow-based averaging techniques were applied to the simulated porosity and permeability for the 128 x 96 grid (the finest grid). The various grids used and their sizes are presented in Table 1. Two programs were used: "powavg" and "flowsim". To compare the results of the two averaging methods, only the results from the first realization of the geostatistical simulation were used. Figure 3 shows permeability distributions obtained from power averaging for 8 x 6 and 32 x 24 grids. A crossplot of the results from the two methods in the x and z directions for 8 x 6 grid are shown in Figures 4 as an example. The purpose of these figures is to determine the correlation coefficients. A correlation coefficient of 1 corresponds to a perfect linear relationship. If there is a perfect correlation, all the points should fall on the 45° line. The averaged values show almost perfect correlation with correlation coefficients ranging from 0.98 to 0.999. It should be noted that the finer the grid, the better correlation coefficients.

To compare how the averaged permeability affects the flow performance of the reservoir, a flow simulation using Eclipse was carried out on an 8 x 6 grid. All three mobility cases were simulated. The results for this simulation can be seen graphically in Figures 5-a oil rate plot. The results obtained using the two averaging methods are very similar in character, especially for M = 0.4 and 1.8. Based on the results presented above, it can be concluded that the power averaging method, even though more approximate, gives results comparable to those obtained using flow simulation. The power averaging results can be improved by adjusting the exponent ω. Thus, permeability averaging can be done quickly and simply by using the power averaging method.

In this study, one hundred (100) realizations obtained using geostatistical modeling were scaled up using the flow-based averaging method. The results of this operation were used for flow simulation of all one hundred realizations.

RUNNING ECLIPSE WITH MULTIPLE REALIZATIONS

The results from all hundred Wingslib simulation realizations were used in Eclipse. There were five grids to be simulated (Table 1). The purpose of running so many realizations was to evaluate the uncertainties in flow simulation results associated with gridding, and with the nature of the

fluids (viscosity-mobility ratios) in the presence of realistic geological heterogeneities. One hundred realizations were used because, with such a number, reasonably reliable statistics of the flow parameters could be inferred. The decision was based on the central limit theorem which states that the uncertainty in calculated statistics is proportional to the uncertainty in one component divided by the number of components [5]. If the number of components (realizations) is 100, as in this study, the uncertainty in the calculated statistics will be only one one-hundredth of the uncertainty in the results of one realization. The permeability now has a different value in each of the three directions, PERMX, PERMY and PERMZ.

Several flow parameters were observed. Among them were the "oil rate", "water rate", recovery factors and water cuts. All parameters were plotted against pore volumes of water injected (PVWI). For all 100 runs of every grid and mobility ratio, the recovery factors at 1 PVWI and breakthrough times were extracted.

This series of plots was constructed for all of the grids and mobility ratios. An example of the plots of oil rate versus PVWI is shown in Figure 6 for 8 x 6 grid. This is an illustration of how the uncertainty in geological modeling through multiple simulation realizations is transferred into the uncertainty in reservoir flow responses. From Figure 6, it can be seen that for the favorable mobility ratio, M = 0.4, the oil rate at the beginning increases sharply (the highest rates were seen after the first time step at $\approx 12,000 sm^3$/PVWI), then drops and flattens out for some time (at rates approximately from 8,000 to 10,000 sm^3/PVWI). At the end, the oil rate gradually decreases. Some realizations can stop earlier, when the oil flow rate fell below the restriction of $1 sm^3$/day. During the period of constant flow, the oil rates show the widest range of difference. After the constant rate period, the oil rate drops gradually, because the reservoir was gradually being swept out. For the unit mobility ratio and the unfavorable mobility ratio cases, the oil rate pattern remains the same, except that there were no peaks at the beginning. The oil rates after the first time step were smaller than those of the following time steps. The period of constant rate was also shorter.

UNCERTAINTY IN RESERVOIR RESPONSE DUE TO GRIDDING AND REALIZATIONS

In order to compare quantitatively the flow performances of the different realizations, for every grid size and mobility ratio, the oil recovery factors at 1 PVWI were recorded. The ranges of the RF for different values of M did not overlap (for M =0.4, the RF range is 0.57-0.63; for M =1 the range is 0.48-0.56; and for M = 1.8, the range is 0.33-0.41). Based on statistics of RF values, a box plot of the RF was drawn, where the maximum, mean, minimum, upper and lower quartiles values are shown (Figure 7). A line was drawn through all the means. This plot reveals that, for every mobility ratio set of results, the mean decreases as the number of cells increases.

If one takes a 128 x 96 grid (the finest) as the most accurate result, and calculates the difference between the RF mean of the 128 x 96 grid and the mean of the RF of the other grids within each M group, it turns out that the 8 x 6 grid is farthest from the reference point (up to 7%). The M =1.8 series shows the most difference between the grids, followed by M = 0.4 and 1.

Similarly to the RF, a box plot of BT is shown in Figure 8. There are distinctive ranges in the BT values for the three mobility ratios. For M = 0.4, the PVWI range is 0.3-0.43; for M = 1, the PVWI range is 0.19-0.32; and for M = 1.8, the PVWI range is 0.08-0.17. Unlike that for the RF, the BT box plot shows diversity in character. The mean line increases for the 8 x 6 to 34 x 24 grids, but then stays the same or decreases for the 64 x 48 and 126 x 96 grids. With the BT's mean for the 128 x 96 grid as a reference point, the highest difference in the mean is for the 8 x 6 grid, M = 0.4 (9 %). Except for the favorable M curve, which shows a clear tendency for the mean to increase as the grid gets finer, there is no clear trend for M = 1 or for M = 1.8.

From the Eclipse simulation results for one hundred realizations and different discretizations, it can be seen that there is uncertainty in the key reservoir performance parameters. This uncertainty is caused by different factors: uncertainty due to the lack of data (different reservoir models from different geostatistical realizations), discretization (related with scaling), and the nature of fluids in the reservoir (different mobility ratios). The question now is how these factors contribute to the overall uncertainty during reservoir simulation. In other words, how quantitatively the overall variability in simulation of reservoir performance parameters is caused by the variability related to these factors. Analysis of variance (ANOVA) is a statistical technique to help to quantify the contribution of different factors to the total variability of the parameters of interest.

The basic problem to which ANOVA is applied is the determination of which part of the variation in the population is due to systematic reasons (called factors) and which part is due to chance [6]. Scheffe [7] defines ANOVA as a statistical technique for analyzing measurements that depend on several kinds of effects operating simultaneously to decide which kinds of effects are important and to estimate the magnitude of these effects. Depending on the number of factors, analysis of variance gives rise to one-way (single factor), two-way (two-factor) or multiple factor models. As it was mentioned before, the recovery factors at 1 PVWI and the breakthrough times were recorded and analyzed. In this part, ANOVA will be applied to these two parameters.

Single factor model for recovery factors at 1 PVWI: In this model, the discretization is considered to be a factor. The variability of the RFs between realizations is the variability within a group. Figure 9 illustrates the contribution of the different sources of variation for the different mobility ratio cases. From Figure 9, it can be seen that the total variation in RFs is biggest for the mobility ratio case of 1 (0.129) and smallest for the favorable mobility ratio case (0.081). In all three mobility ratio cases, the variation due to discretization is smaller than the variation due to different realizations. If the relative contribution of two sources is compared, it can be seen that the discretization effect contributes less to the total variation in the case of the mobility ratio of 1 (about 16%) followed by the case of mobility ratio of 0.4 (about 42%) and M = 1.8 (about 43%).

The reason why the variability in the RFs is less due to discretization, and more due to the realization, for the unit mobility ratio case is probably, for this mobility ratio, there is a no-win situation where there is no dominant flow of either water or oil. Different realizations with different spatial continuity become more important in determining the flow paths of the fluids in a reservoir. Therefore, the variation due to different realizations contributes more to the total variation in the recovery factors at 1 PVWI.

Single factor model for breakthrough times: Similar to the RF case, ANOVA for the BT parameter was implemented. The factor is the discretization. A mobility ratio case of 1.8 has the smallest variation of BTs (0.091), followed by M = 1 (0.325) and M = 0.4 (0.333). The proportion of the variation due to discretization is 26, 7 and 11% for M = 0.4, 1 and 1.8, respectively. Again, the percentage is smallest for the mobility ratio of 1. The reason for this observation can be explained similarly to that for the ANOVA for the RFs.

The results of the ANOVA analysis mentioned above were obtained from the 2-D reservoir model. One should be very careful to infer these results to the 3-D reservoir model because the behavior of the fluid flow in 3-D model is more complicated than in the 2-D model. The same results may not be observed for the 3-D model.

RANKING BASED ON FLOW SIMULATION RESULTS

In order to assess the uncertainty in geological model and therefore in reservoir flow parameters, a large number of geological (or realizations) are constructed. The full flow simulation approach means flow simulation for all the realizations in very fine grids, with very large CPU time. An

option to reduce the computational effort is to use different ranking techniques. The central idea behind ranking realizations is to use some simpler measure to rank realizations and then run the full flow simulation with fewer realizations, say the 5%-low, 50%-expected and 95%-high ones. This would allow bounding the uncertainty without performing a large number of fine-scale flow simulations. A simpler measure is a good ranking statistic when it correctly identifies low and high realizations [8]. Realization rank is scenario dependent. Ideally, a ranking methodology would lead to the same rank obtained with the flow response of interest [9].

Almost all flow parameters depend on some measure of continuity, connectivity or tortuosity. The ranking tools increase in complexity and require knowledge of the specific problem. More information must be known about the reservoir and production plan to rank realizations based on the more complex ranking measures. In the literature up to date, there are two main ranking technique groups: ranking with statistical measures based on simple summary statistics and ranking with simple fast flow model.

For the fast flow simulation technique, recovery factors and breakthrough times were considered for ranking. For every grid discretization and mobility ratio case, values of these flow responses were ranked from the highest (rank number 1) to the lowest (rank number 100).

The flow simulation results are assumed to be the most accurate (closer to the true) for the finest 128 x 96 grid. The ranking results of coarser grids were crossplotted against the ranking of the 128 x 96 grid. Figure 10 illustrates these crossplots for RFs, M = 0.4. The straight line represents perfect correlation (correlation coefficient of 1). The general observation is that the finer becomes the grid, the closer are plotted points to the perfect correlation line. The correlation coefficients from ranking crossplots were plotted in Figure 11. From figure 11, it can be seen that as a grid gets finer, the correlation coefficients increase closer to 1. The range of correlation coefficients for the RFs is from 0.59 to 0.99, and for the BTs from 0.38 to 0.85. The correlation coefficients for the RFs are higher than for the corresponding values for the BTs. The correlation coefficient curves for different mobility ratio cases are very close together except the one for the RF of the case of M = 1. It goes from a relatively low value of 0.59 for 8 x 6 grid to a value of 0.89 for the next finer 16 x 12 grid and departs from the other two curves for the RFs.

The conclusion to be drawn based on the correlation coefficients between the coarser grids and a very fine grid is that the RFs and BTs of the reservoir can be fairly predicted based on the simulation results of a very coarse grids.

CONCLUSIONS

Grid discretization effects must always be considered in reservoir simulation. The magnitude of the discretization effects is different depending on the porosity-permeability properties of the reservoir: homogenous or heterogeneous, downscaling or upscaling. Grid discretization effect also depends on the nature of the fluid in the reservoir. Recovery factors has more predictable behavior than breakthrough times for different fluid types. This study shows that upscaled permeability values of the reservoir using power and flow-based techniques give very close reservoir flow responses.

Another conclusion from this study is that it is important to recognize and assess quantitatively sources of uncertainty in reservoir modeling. Uncertainty in geological modeling contributes more to the total uncertainty than the grid discretization, therefore as many geological realizations as possible should be used in flow simulation during reservoir study. Ranking different geological realizations before running flow simulation on a fine scale can be used as a tool to compromise computing resources and the task of uncertainty assessment. Recovery factors from flow simulation of a very coarse grid can be used as a fair to good ranking parameter to assess the uncertainty in reservoir flow simulation.

The procedure used in this study for reservoir uncertainty assessment is not only confined to academic purpose, but can be applied to any practical reservoir study. The results of quantitative uncertainty assessment will be important in reservoir management and decision making.

REFERENCES

1. Settari, N.G. and Toronyi, R.M., 1988. Engineering control in reservoir simulation. SPE Paper Number 18305.

2. Journel, A.G., Deutsch, C., Desbarats, A.J., 1986. Power averaging for block effective permeability. SPE Paper Number 15128.

3. Deutsch, C., 1986. Estimating block effective permeability with geostatistics and power averaging. SPE Paper Number 15991.

4. Li, D., Beckner, B., 1999. A new efficient averaging technique for scaleup of multimillion-cell geologic models. SPE Paper Number 56554.

5. Deutsch, C., 1999. Geostatistical methods for modeling earth science data, lecture notes.

6. Massart, D.L., Vandeginste, B.G.M., Deming, S. N., Michotte, Y., Kaufman, L., 1988. Chemometrics: a textbook, Elsevier, New York.

7. Scheffe, H., 1959. The analysis of variance, Wiley, New York.

8. Ballin, P.R., Aziz, K., Journel, A. G., 1993. Quantifying the impact of geological uncertainty on reservoir performing forecast. SPE Paper Number 25238.

9. Deutsch, C., Srinivasan, S., 1996. Improved reservoir management through ranking stochastic reservoir models. SPE Paper Number 35411.

Grids	Number of cells	Dx (m)	Dy (m)	Dz (m)
8 x 6	48	75	1	16.6667
16 x 12	192	37.5	1	8.3333
32 x 24	768	18.75	1	4.1667
64 x 48	3072	9.375	1	2.0833
128 x 96	12288	4.6875	1	1.0417

Table 1: Different reservoir discretizations for the heterogeneous reservoir case

Grids	Number of cells	Dx (m)	Dy (m)	Dz (m)
7 x 5	35	100	1	20
16 x 12	192	40	1	8.33
31 x 25	775	20	1	4
61 x 50	3050	10	1	2
121 x 100	12100	5	1	1
241 x 200	48200	2.5	1	0.5
481 x 400	192400	1.25	1	0.25

Table 2: Different reservoir discretizations for the homogeneous reservoir case
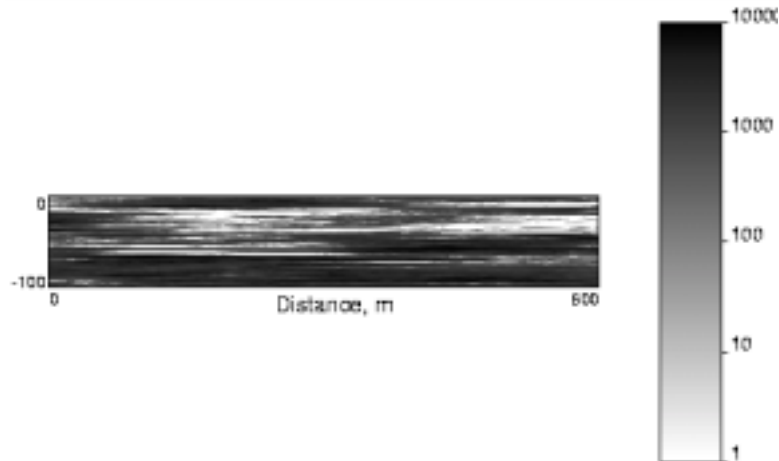
Figure 1: Grid 128 x 96, realization 1: permeability distribution
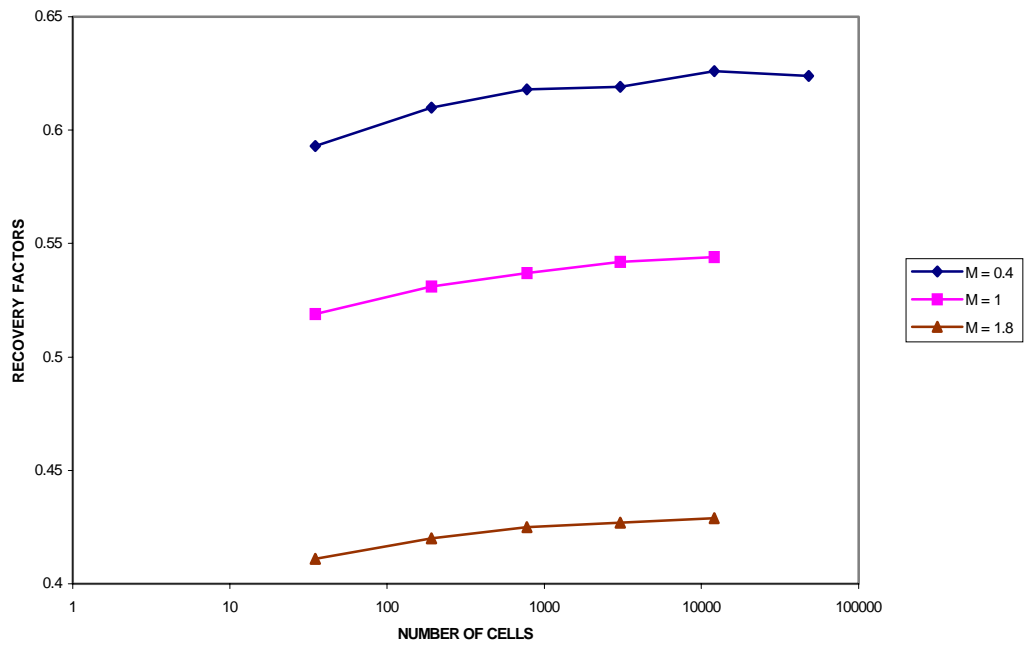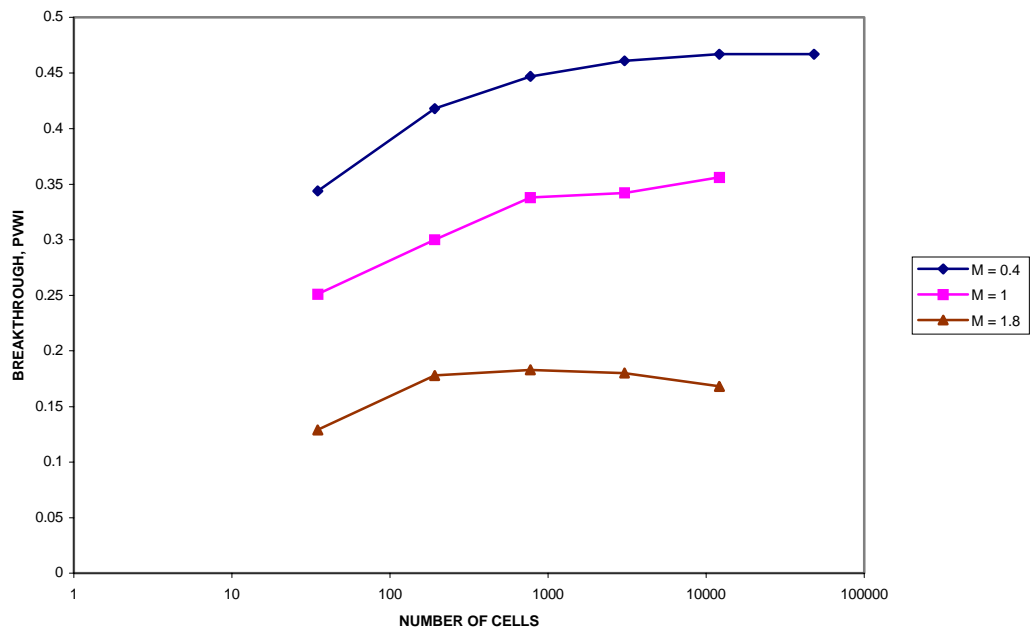
Figure 2: (a) Recovery factors at 1 PVWI for different discretizations and mobility ratios - homogeneous reservoir. (b) Breakthrough times taken at ≈ 0.01 water cuts for different discretizations and mobility ratios - homogeneous reservoir

Figure 3: Permeability distribution obtained from power average technique for (a) 8 x 6 and (b) 32 x 24 grids (see scale of Figure 1)

11
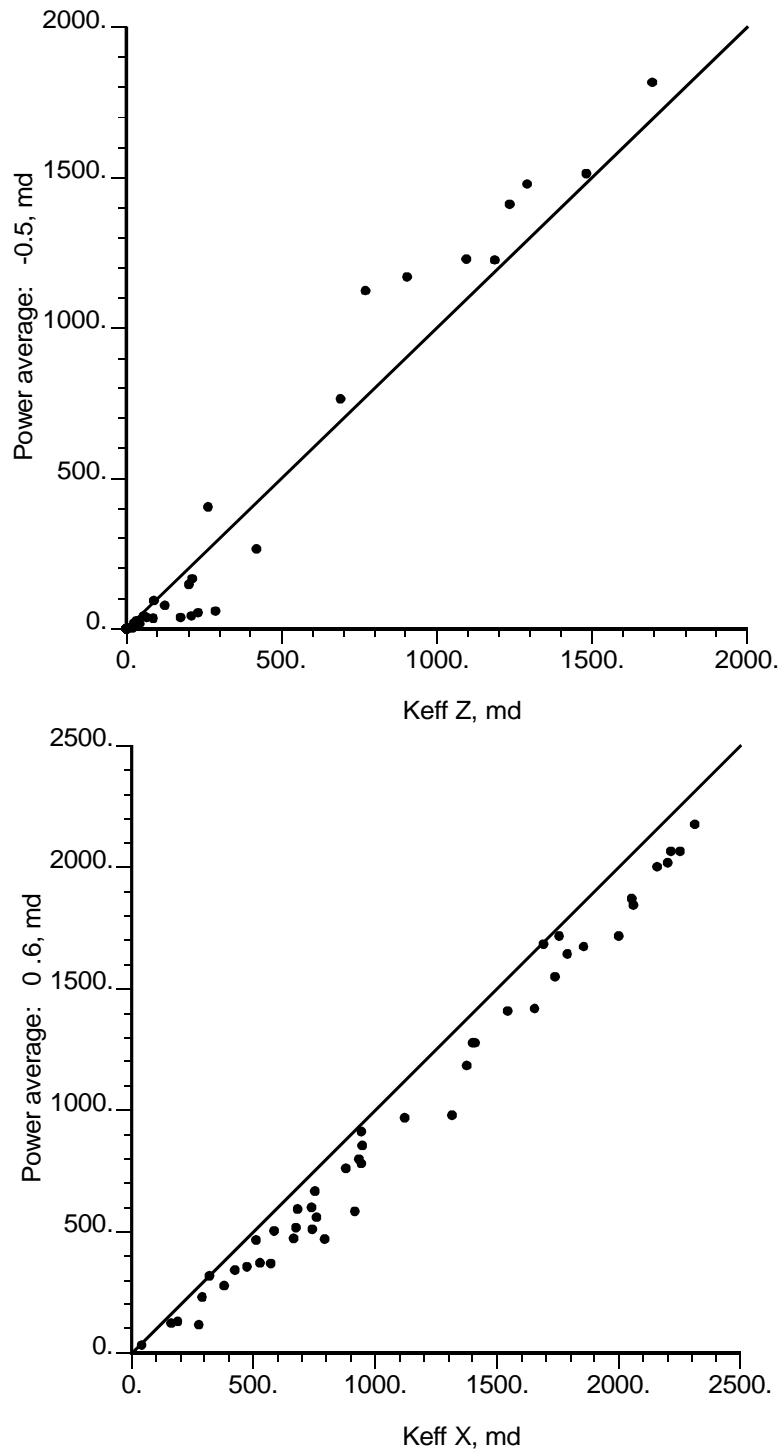
Figure 4: (a) 8 x 6 grid – effective versus power averaged permeability in x direction; (b) 8 x 6 grid – effective versus power averaged permeability in z direction
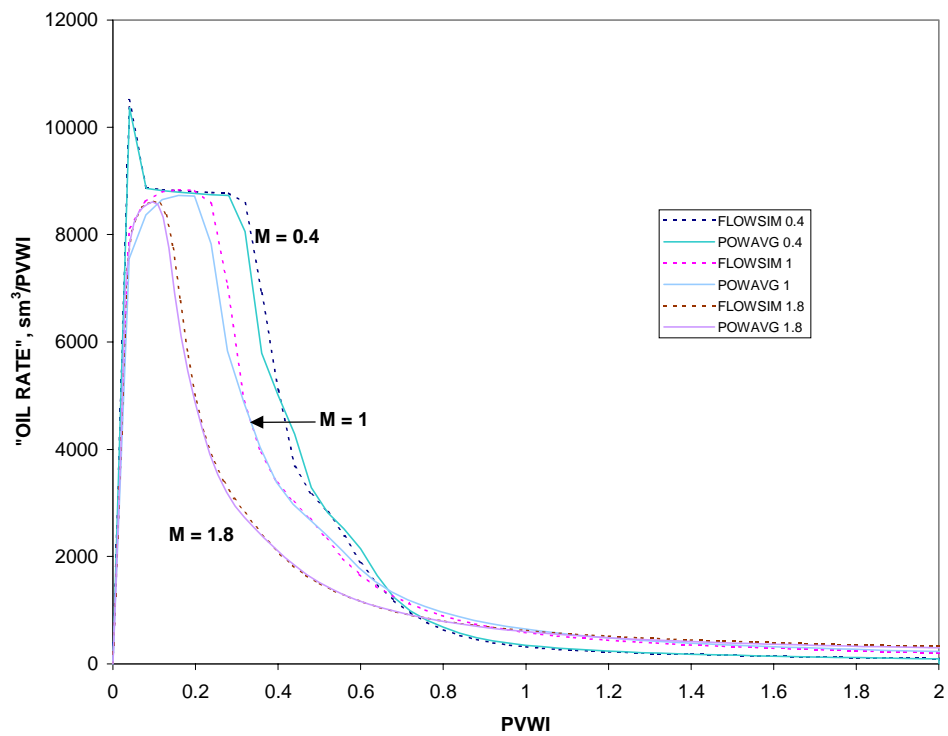
Figure 5: 8 x 6 grid – "Oil production rates" using permeability averaged by power law and flow-based techniques
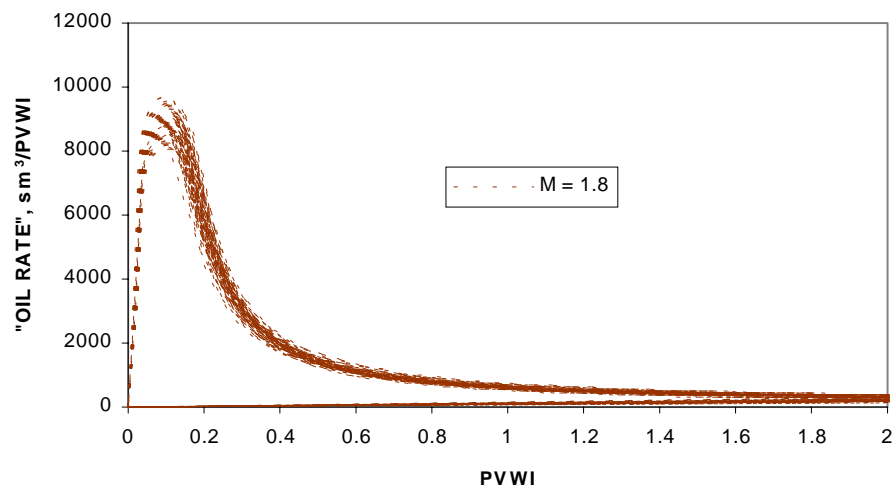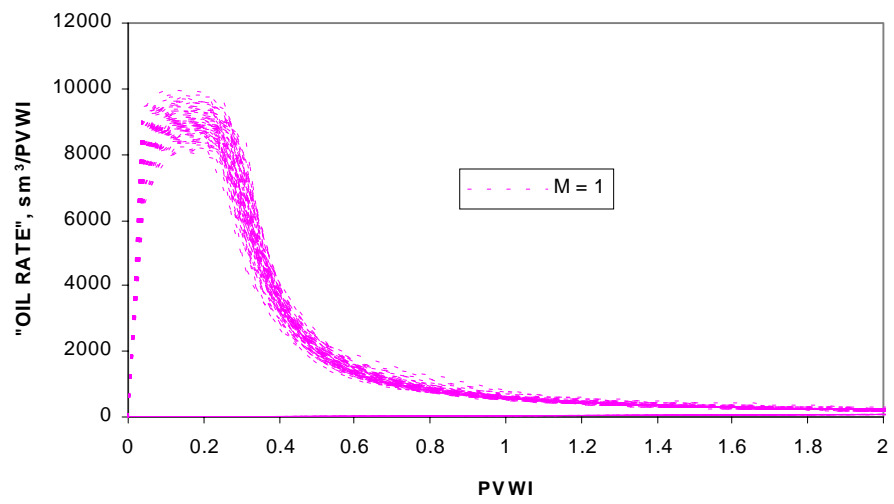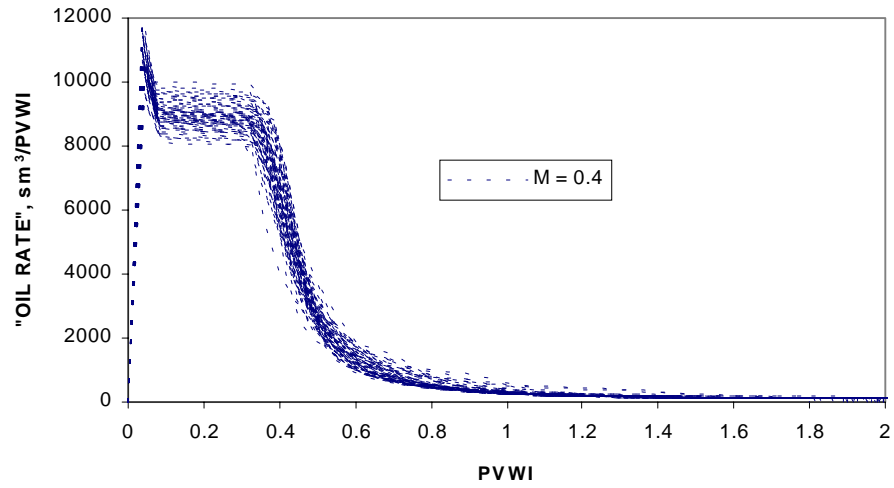
Figure 6: "Oil rates" versus PVWI for 100 realizations , 8 x 6 grid
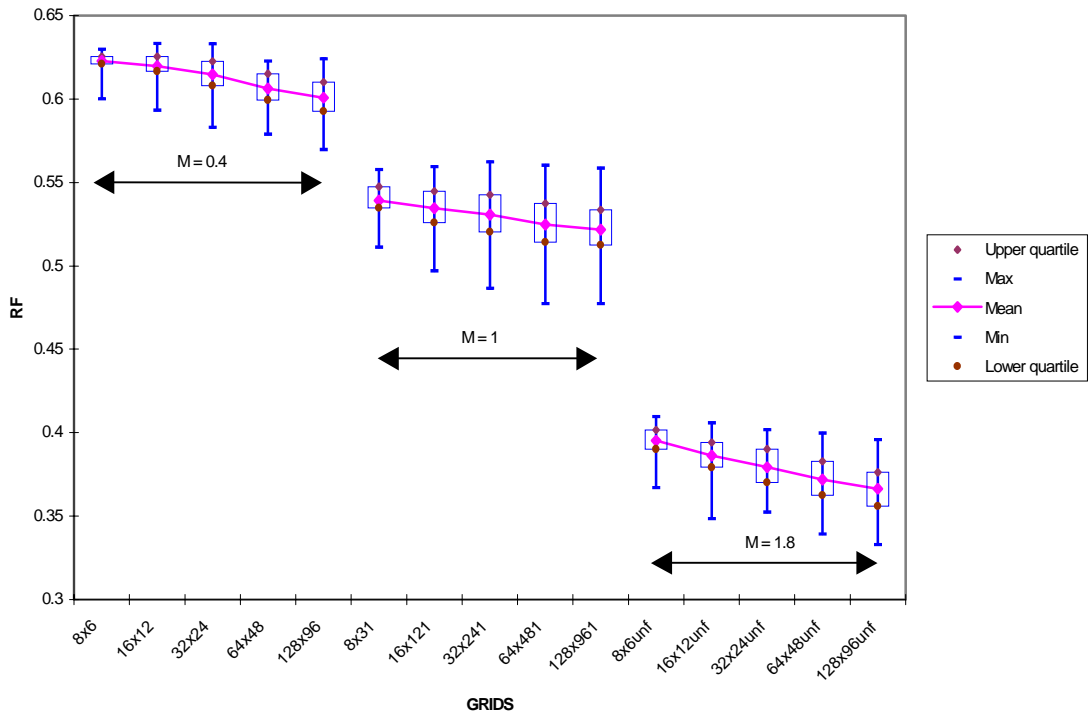
Figure 7: Box plot of recovery factors measured at 1 PVWI for different grids and M
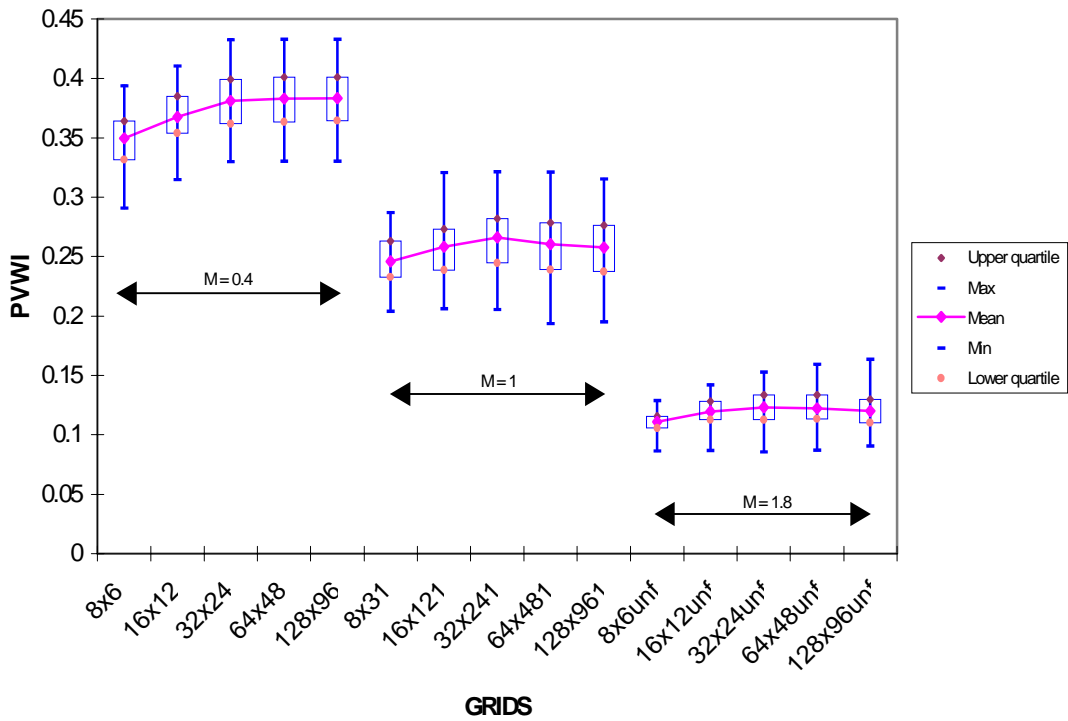
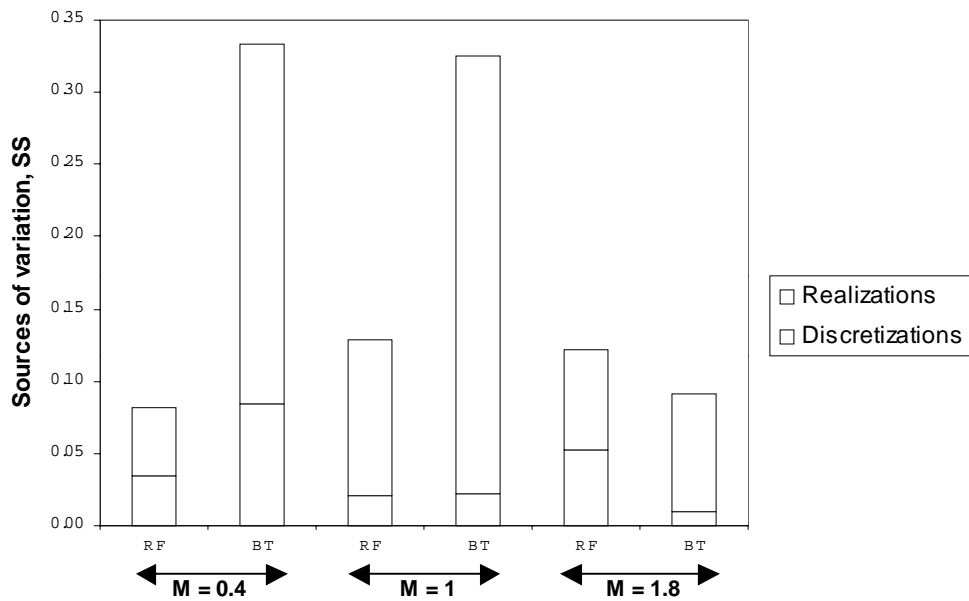Figure 8: Box plot of breakthrough times for different grids and mobility ratios

Figure 9: Single factor ANOVA for recovery factors at 1 PVWI and breakthrough times
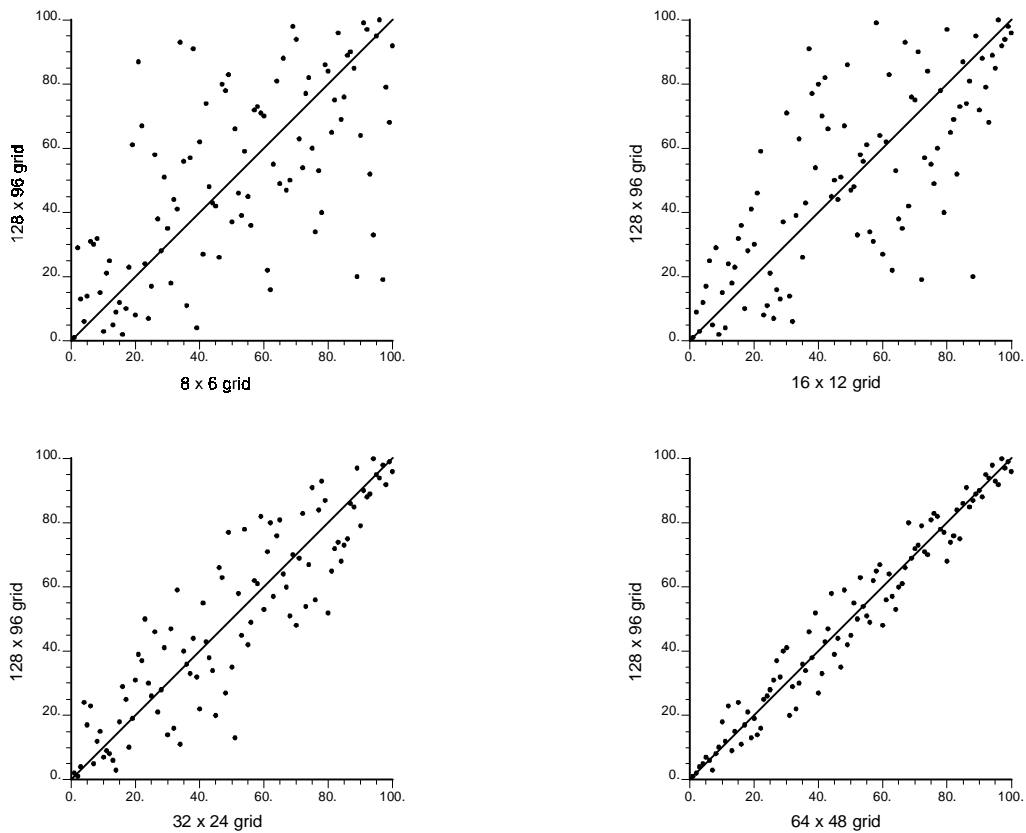

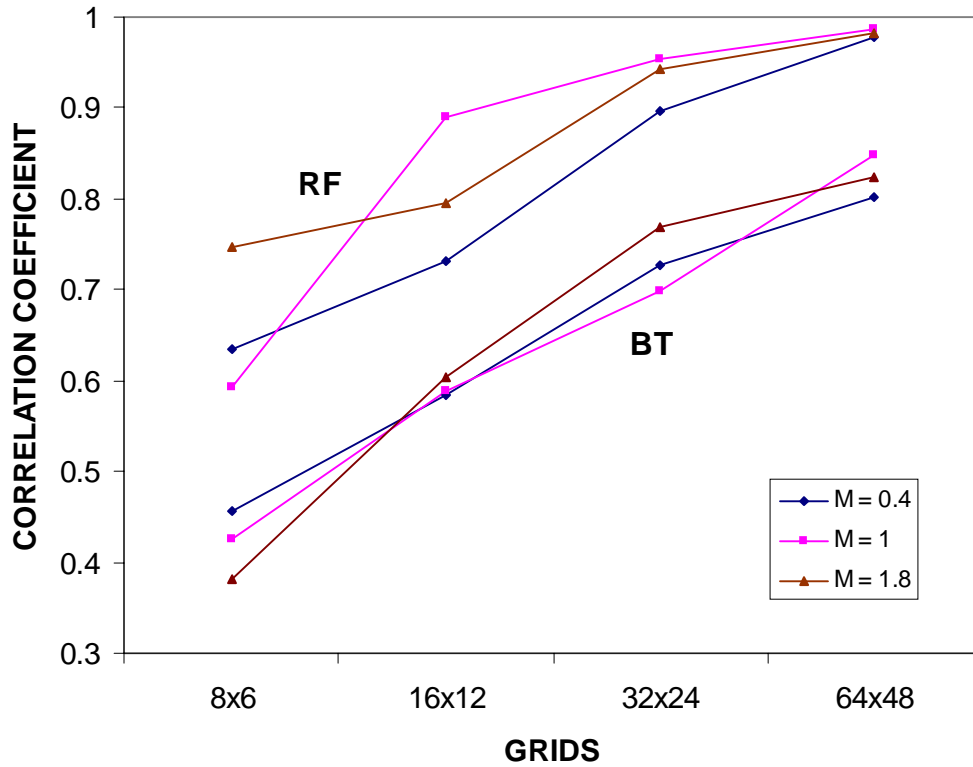Figure 10: Crossplot of ranking numbers of RFs for different grids, M = 0.4

Figure 11: Correlation coefficients between recovery factors and breakthrough times of 128 x 96 and of coarser grids